

Experimental Study of the Generation of Periodic Internal Waves by the Boundary Layer on a Rotating Disk

Yu. D. Chashechkin, Yu. V. Kistovich, and Yu. S. Il'inykh

Presented by Academician A. Yu. Ishlinskiĭ February 10, 2000

Received February 11, 2000

The exact solution to the linearized problem of the generation of internal waves, which involves internal waves and internal boundary flows [1], allows us to estimate errors intrinsic to the well-known method of force (or mass) sources [2]. In the case of small displacements, calculations of perturbances excited by an oscillating bar satisfactorily agree with the measurement results of [3]. There exist situations when a body moving periodically in continuously stratified viscous fluid does not radiate (in the linear case) and generates only isopycnic boundary flows. This situation takes place, e.g., in the case of a horizontal disk performing torsional vibrations [4]. However, by virtue of the nonlinear nature of the hydrodynamic system of equations, various forms of motion interfere with one another. In particular, thin-layer boundary flows can be a source of periodic waves [4]. Previously, experimental studies of such internal-wave generators were not conducted. Therefore, it is of interest to investigate the practical feasibility of the principles for nonlinear generation. In the present paper, the possibility of generation of three-dimensional beams of periodic internal waves by torsional vibrations of a horizontal disk are studied and the principal regularities connecting wave-field characteristics with the properties of a medium and source motion parameters are established.

The experiments were performed in a laboratory wave channel with dimensions $9.0 \times 0.6 \times 0.6$ m filled with an exponentially stratified solution of common salt, which had transparent windows made of optical glass. The period (for the frequency N) of the buoyancy

$$T_b = \frac{2\pi}{N} = 2\pi \sqrt{\frac{\Lambda}{g}},$$

where $\Lambda = \left(\frac{d \ln \rho_0}{dz}\right)^{-1}$ is the stratification scale, $\rho_0(z)$ is the density profile, and g is the free-fall acceleration,

was determined by the density tag method [5] and was found in our experiment to be $T_b = 7.5$ s. Observations of the flow pattern in the vertical plane were performed by the shadow IAB-451 device using the method called “the vertical slit-thread in focus” [6]. Due to the symmetry of the flow pattern in the linearly stratified medium, the shadow device visualizes the perturbation distribution in the central vertical axis, where the light beam passes along the tangent to the wave phase surfaces. The rest contributions initiated by perturbances along the beam are mutually compensated. The measurements of wave displacements were carried out by an electrical-conduction single-electrode sensor and using sweep-vibration methods [7]. The sensor was calibrated before each experiment in accordance with the lifting-submersing procedure. The error of wave-displacement measurement did not exceed 20%.

The wave source was a horizontal disk 1 mm thick and 2 (or 4) cm in diameter. The disk was fixed to a vertical rod 2 mm in diameter, which was connected through a reducer to a dc motor. To reduce perturbances of the medium, the rod was placed in an immobile tube 6 mm in diameter. Adjustment of the rotation frequency and the law of disk motion was performed by varying the voltage applied to the motor. The angular displacement of the motor was recorded by a multiturn potentiometer. Three types of disk motion were studied: torsional harmonic vibrations (with the angular velocity $\Omega = \Omega_0 \sin \omega^* t$); intermittent alternate rotations (meander)

$$\Omega = \Omega_0 \begin{cases} +\Omega_0, & nT < t < nT + \frac{T}{2} \\ -\Omega_0, & nT + \frac{T}{2} < t < nT + T, \end{cases}$$

where $T = 2\pi/\omega^*$; and harmonic torsional vibrations against the background of a uniform rotation ($\Omega = A + \Omega_0 \sin \omega^* t$). The maximum linear velocity for the disk edge motion was $U = 10$ cm/s.

The flow shadow pattern appearing after the completion of two 4-cm-disk vibrations is shown in Fig. 1. Among the optical inhomogeneities of the pattern, we

Institute of Problems in Mechanics,
Russian Academy of Sciences,
pr. Vernadskogo 101, Moscow, 117526 Russia

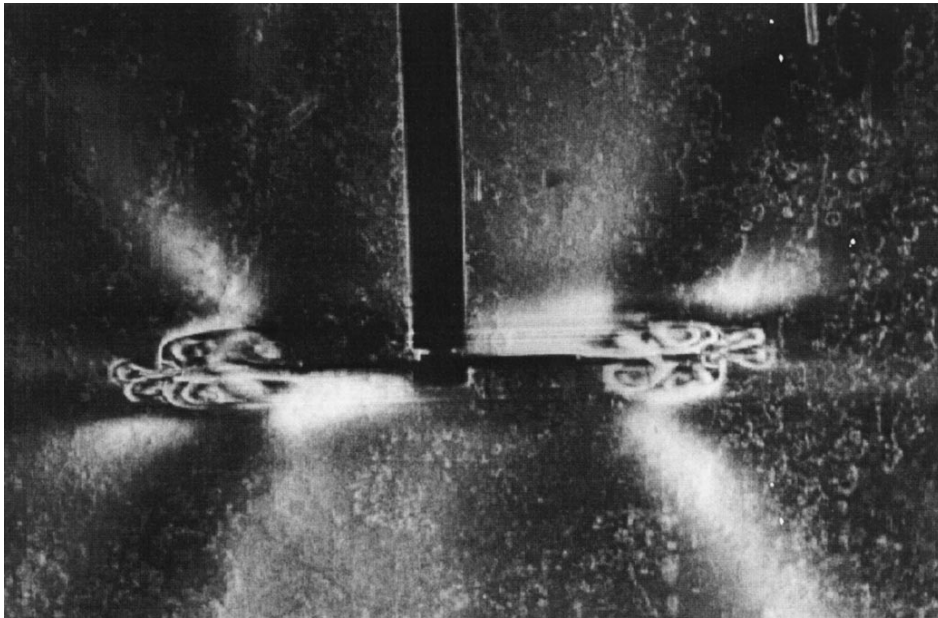


Fig. 1. Shadow pattern of a flow formed by a horizontal disk performing torsional vibrations; $T_b = 7.5$ s, $T = 20$ s, $U = 2$ cm/s.

can distinguish a sequence of thin strips positioned in parallel to the disk, which are linked by three embedded ring-shaped structures. Two systems of inclined, almost horizontal, diffusive dark and light strips branch out of the external surface of the layered structure. In the upper half space, the interior strip is dark, whereas in the lower one, the opposite situation takes place. Horizontal strips are antisymmetric to both the right and the left. The positions of the horizontal interlayers, as well as the size and shape of the vortices linking these interlayers, and the mutual positions of the dark and light inclined strips vary with time.

Comparison with the results of [3, 8] for shadow observations of stratified flows shows that inclined diffusive strips represent schematically periodic internal waves with frequency $\omega = 2\omega^* = 0.62$ s⁻¹, which propagate at an angle $\theta = 47^\circ$ to the horizon, as well as diffusive horizontal strips, i.e., waves of the zero frequency, and high-gradient interlayers, i.e., shells of rotating ring-shaped flows at the disk edge. The distribution of optical perturbances in the shadow image, when the blackening density is determined by the horizontal component of the refractive index (or the density) bound by the linear relationship [8], testifies to the existence of an antisymmetric pattern of periodic waves: a crest in the upper half space corresponds to a hollow in the lower one and vice versa.

Observations of the flow pattern show that at the initial phase of the flow, boundary flows arise at both disk sides; each of these flows forms a circular flow rotating together with the disk, the cross section of this flow having an annular shape. The large and small ring radii monotonically increase with time up to the moment of changing the rotation direction. At this moment, the

flow separates from the disk and begins to attenuate. As far as the ring-shaped flow is being damped, its vertical dimension decreases and its vortices collapse. In the case of changing the rotation direction (at every half of a period), a new pair of boundary flows and, correspondingly, a pair of new monotonically raising annular flows arise. In each of these flows, the fluid takes part in two types of rotary movement, namely, around the vertical disk axis in the horizontal plane and in the vertical plane around the circular symmetry axis. As in the uniform medium, the disk forms the middle flow [9], in which the fluid flows along the vertical axis and is thrown away in the disk plane forming a wave beam of zero frequency in the stratified medium. The direction of the middle flow induced by the disk is independent of its rotation direction.

In the shadow pattern (Fig. 1), we observe traces of three pairs of annular flows. The first (outer) flow pair has collapsed under the action of buoyancy forces; the second (central) pair has a clearly expressed annular structure similar to the vortex structure in a homogeneous fluid [10]; and the third pair intervenes in them. The external boundaries of annular flows are seen above and below the disk as thin horizontal interlayers. Their thickness does not exceed 0.3 mm and, in fact, is determined by the resolution of the shadow device [6]. The shape of the exterior annular flow demonstrates that the mixing of the fluid inside this flow is weak, since its fragments come to the disk horizon within the observation time.

The outer boundary of annular flows being formed near the disk radiates two groups of axisymmetric periodic internal waves at a frequency $\omega = 2\omega^*$. These waves propagate at an angle $\theta = 47^\circ$ to the horizon. Fur-

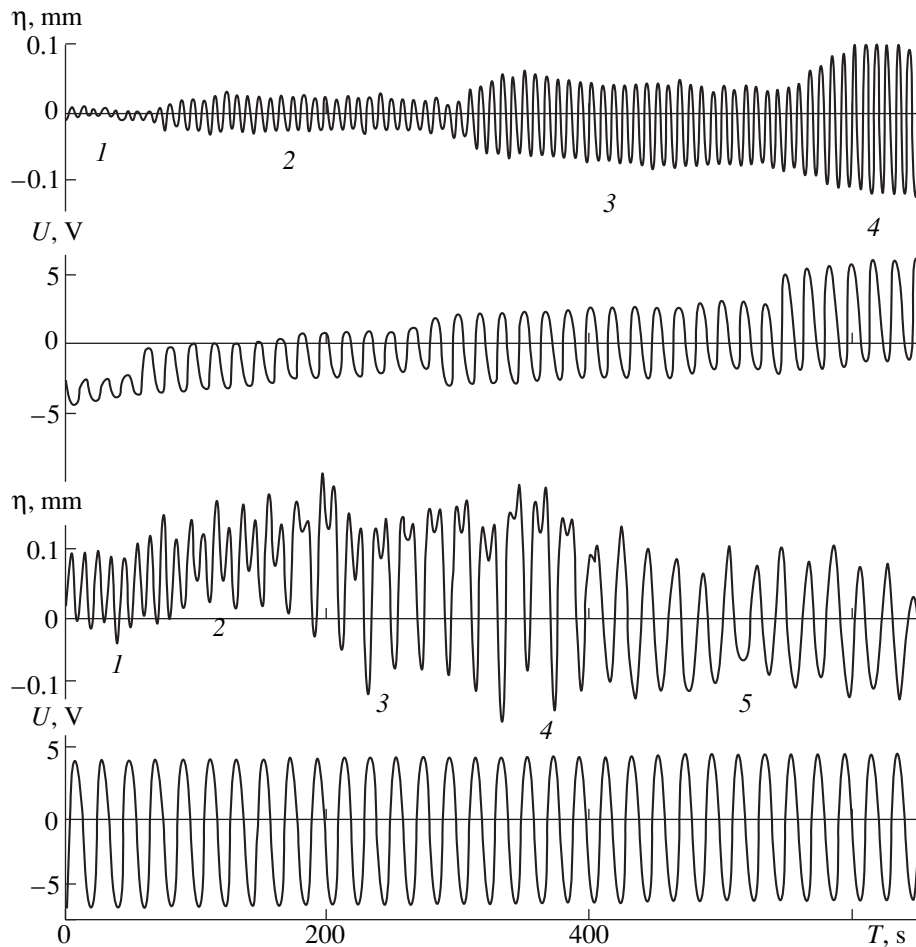


Fig. 2. Recorded signals of electrical-conductance and disk position sensors.

thermore, all elements of this pattern are repeated in every half of a period and the common-rotation direction of annular vortices in the horizontal plane changes.

The signals registered from the electrical-conductance sensor installed in the internal-wave beam at a distance of 8 cm from the disk (the sensitive element of the sensor is depicted in the upper right angle of Fig. 1) are shown in Fig. 2. In the same figure, the signals from the disk angular position for which a multiturn potentiometer is used is also presented. The upper pair of records corresponds to the case when the 4-cm disk performs harmonic torsional vibrations at a constant frequency and with different amplitudes [(1-4): $U = 0.4, 1.3, 3.5, \text{ and } 5.8 \text{ cm/s}$]. Stable internal waves are excited at all velocities of disk motion. Comparing the upper pair of records, we can see that the frequency of the radiated wave exceeds that for the torsional vibrations by a factor of two. The small amplitude modulation of the signal is initiated by seiches existing in the basin. The drift of the potentiometer signal with time is caused by the specific asymmetry of the control signal and by features of the motor operation in itself. The internal-wave amplitude increases linearly with the tor-

sional-vibration amplitude [(1-4): $\eta = 0.01, 0/03, 0/06, 0.11 \text{ cm}$].

The lower pair of the records in Fig. 2 corresponds to the case when, in addition to the alternating voltage, the permanent voltage is applied to the motor. The value representing this voltage consequently becomes equal to the harmonic-signal amplitude and, furthermore, exceeds it. In this case, torsional harmonic vibrations of the 2-cm disk ($U \sin \omega^* t$, $U = 2.8 \text{ cm/s}$, $\omega^* = 0.31 \text{ s}^{-1}$) are added to the unidirectional rotation (with velocity values 1-5, respectively, of 0, 1.0, 3.5, 6.0, and 9.8 cm/s) and are gradually transformed into motion with the alternate angular velocity of the constant sign ($U_0 > U$). In the sensor signal which is initially harmonic and has the frequency $2\omega^*$, a noticeable component appears that becomes dominating with further increase in the permanent rotation component (see segment 3). In this case, the energy of emitted waves also increases.

The dependence of the vertical displacements in the internal-wave beam on the maximum velocity of the disk edge in the case of purely torsional vibrations is presented in Fig. 3 (the sensor is placed at a distance of

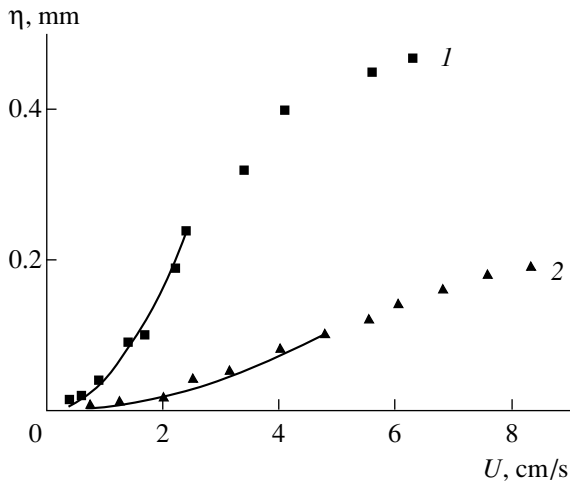


Fig. 3. Vibration amplitudes for particles on the internal-wave beam axis as a function of the disk edge rotation velocity: (1) $D = 4$ and (2) 2 cm.

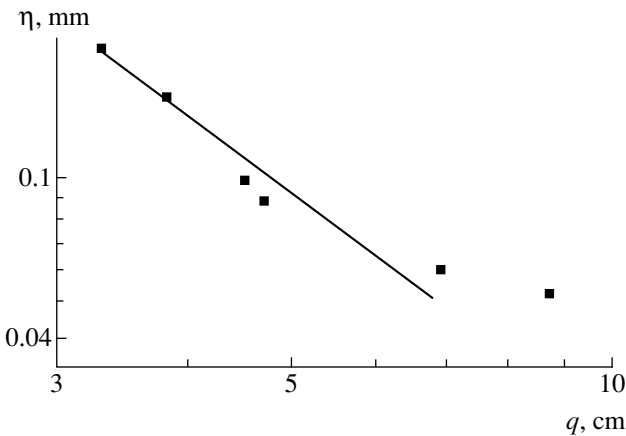


Fig. 4. Vibration amplitude for particles on the beam axis as a function of the distance to the radiator ($T_b = 7.5$ s, $D = 4$ cm, $T = 16.7$ s, $U = 2$ cm/s).

8 cm from the disk along the beam axis). At low rotation velocities of the disk ($U < 3$ cm/s), the wave amplitude increases quadratically for the radiators of both diameters ($D = 2$ and 4 cm: $\eta = 0.005U^2$ and $0.04U^2$; η and U are expressed in millimeters and centimeters per second, respectively, see curves 1 and 2). At intermediate velocities, the amplitude-increase rate is gradually slowed, and for $U > 8$ cm/s, saturation takes place owing to the combined action of the nonlinearity and viscosity effects.

The plot illustrating the attenuation of particle displacement amplitudes at the beam axis as a function of the distance to the radiator is presented in the double-logarithmic scale in Fig. 4. Making use of the least-squares method shows that for $q < 7$ cm, experimental points are grouped around the curve $\eta = 1.14q^{-1.54}$. At longer distances ($q > 7$ cm), the recorded wave amplitude attains saturation (the vertical displacement is on

the order of 0.05 mm) caused by the wave background of the basin. This background is formed due to the action of other independent sources (mechanical vibrations of the ground, as well as vibrations of the base and walls of the basin, which are caused by the action of the wave-producing device). The level of residual vibrations in Fig. 4 corresponds to the modulation depth in Fig. 2.

As was shown in the experiments, the amplitude of the wave being radiated substantially depends on the characteristics of disk motion (under the condition of preserving the frequency and amplitude for its periodic component). When the envelope is a meander, only annular flows and waves are observed in the flow pattern (running internal waves are absent).

As is shown in the theory of the excitation of internal waves by the horizontal disk performing the torsional vibrations in a stratified viscous fluid [4], the true wave source is an isopycnic boundary flow characterized by a single azimuth velocity component u_ϕ . The stream function Ψ for the beam of radiated waves satisfies the equation

$$\left[\frac{\partial^2}{\partial t^2} \left(\Delta - \frac{1}{r^2} \right) + N^2 \left(\Delta - \frac{\partial^2}{\partial z^2} \right) - \nu \frac{\partial}{\partial t} \left(\Delta - \frac{1}{r^2} \right)^2 \right] \Psi = \frac{1}{r} \frac{\partial^2 u_\phi^2}{\partial t \partial z}, \tag{1}$$

where Δ is Laplacian, ν is the kinematic viscosity, and the origin of the cylindrical coordinate system (r, ϕ, z) is taken in the disk center. The solution to this equation with exact boundary conditions describes both running waves [4] and zero-frequency waves. The form of the right-hand side of Eq. (1) implies that the frequency of waves excited by harmonic torsional vibrations of the disk is twice that of their own frequency. The meander squared is a quantity independent of time, which explains the radiative inefficiency of the periodic motion of this type.

It follows from the solution to Eq. (1) that torsional vibrations of a disk whose radius is smaller than the viscous wave scale $L_\nu = \sqrt[3]{g\nu/N}$ excite a single-mode wave beam. The displacements of the particles along the beam axis are

$$h(q) = \frac{U^2 R^2 \sin \theta}{48(1 + \sqrt{2})} \left(\frac{2 \cos^4 \theta}{\pi^3 \nu^4 N^8 q^{10}} \right)^{1/6} \Gamma \left(\frac{7}{6} \right), \tag{2}$$

where Γ is the gamma function and q is the distance along the beam axis to the source. The quadratic dependence of the wave amplitude on the velocity U in (2) is consistent with the measurement data exhibited in Fig. 3. In this theory, the wave amplitude also depends quadratically on the disk radius. The ratio of the coefficients in formulas interpolating experimental data of Fig. 3 is equal to 8, whereas the ratio squared for disk

diameters is 4. This discrepancy is associated with the fact that under the experimental conditions, the waves excite both isopycnic boundary flows and annular rotating vortices. The efficiency of the second generation mechanism that is not taken into account in the theory elevates with increasing disk diameter. The decrease in the beam amplitude with the distance from the source, which is calculated in accordance with (2) under the experimental conditions presented in Fig. 4, is given by the expression $h = 1.29q^{-5/3}$, where h and q are expressed in millimeters and centimeters, respectively. For $q < 7$, empirical data can be approximated by the dependence $h = 1.14q^{-1.54}$. Deviations in the indices (8%) and coefficients (13%) do not exceed the measurement error for the wave amplitudes by the contact electrical-conductance sensor, which attains 20% in the experiments under discussion. Thus, the disk performing high-amplitude torsional vibrations in the continuously stratified fluid efficiently radiates periodic internal waves.

The method described expands the spectrum of possible means for excitation of internal waves including wave generation under the action of viscous stresses [11], as well as by varying the volume and position of a body [12].

ACKNOWLEDGMENTS

This work was carried out under the financial support of the Ministry of Science and Technology of the Russian Federation (in the framework of the Program of Supporting Unique Experimental Facilities) and of

the Russian Foundation for Basic Research, project no. 99-05-64980.

REFERENCES

1. Yu. D. Chashechkin and Yu. V. Kistovich, Dokl. Akad. Nauk **355**, 54 (1997) [Phys. Dokl. **42**, 377 (1997)].
2. M. G. Lighthill, *Wave in Fluids* (Cambridge Univ. Press, Cambridge, 1978; Mir, Moscow, 1981).
3. Yu. S. Il'inykh, Yu. V. Kistovich, and Yu. D. Chashechkin, Izv. Akad. Nauk, Fiz. Atm. Okeana **35**, 649 (1999).
4. Yu. V. Kistovich and Yu. D. Chashechkin, Dokl. Akad. Nauk **367**, 636 (1999) [Dokl. Phys. **44**, 573 (1999)].
5. S. A. Smirnov, Yu. D. Chashechkin, and Yu. S. Il'inykh, Izmer. Tekh., No. 6, 15 (1998).
6. L. A. Vasil'ev, *Schlieren Methods* (Nauka, Moscow, 1968; Israel Program for Scientific Translations, Jerusalem, 1971).
7. A. V. Gvozdev, V. I. Neklyudov, and Yu. D. Chashechkin, Izmer. Tekh., No. 3, 33 (1990).
8. D. E. Mowbray, J. Fluid Mech. **27**, 595 (1967).
9. H. Schlichting, *Theory of Boundary Layers* (McGraw-Hill, New York, 1955; Nauka, Moscow, 1960).
10. *Album of Fluid Motion*, Ed. by M. VanDyke (Parabolic Press, Stanford, 1982; Mir, Moscow, 1986).
11. A. V. Kistovich and Yu. D. Chashechkin, Prikl. Mekh. Tekh. Fiz. **40** (6), 31 (1999).
12. S. A. Makarov, V. I. Neklyudov, and Yu. D. Chashechkin, Izv. Akad. Nauk SSSR, Fiz. Atm. Okeana **26** (7), 744 (1990).

Translated by G. Merzon